Process Biochemistry 47 (2012) 1933–1943

Contents lists available at SciVerse ScienceDirect

Process Biochemistry

journal homepage: www.elsevier.com/locate/procbio

Protein stabilizing potential of simulated honey sugar cocktail under various denaturation conditions

Yin-How Wong, Saad Tayyab*

Biomolecular Research Group, Biochemistry Programme, Institute of Biological Sciences, Faculty of Science, University of Malaya, 50603 Kuala Lumpur, Malaysia

ARTICLE INFO

Article history:
Received 7 March 2012
Received in revised form 26 June 2012
Accepted 26 June 2012
Available online 4 July 2012

Keywords:
Simulated honey sugar cocktail
Protein stabilization
Urea denaturation
Bovine serum albumin

ABSTRACT

Protein stabilizing potential of simulated honey sugar cocktail (SHSC) against chemical and thermal denaturations was studied using bovine serum albumin (BSA) as the model protein. The two-step, three-state transition of urea denaturation of BSA became a single-step, two-state transition along with the shift in the whole transition curve towards higher urea concentrations in the presence of increasing SHSC concentrations [8–20% (w/v)] as revealed by far-UV CD, fluorescence and UV difference spectroscopic results. Far-UV and near-UV CD spectra, UV difference spectra, ANS fluorescence and three-dimensional fluorescence results suggested significant retention of native-like conformation in 4.6 M urea-denatured BSA in the presence of 20% (w/v) SHSC. A significant shift was also noticed in thermal and GdnHCl denaturation curves of BSA in the presence of 20% (w/v) SHSC. Taken together, all these results suggested significant stabilization of BSA against urea, GdnHCl and thermal denaturations by SHSC.

1. Introduction

Over the past 40 years, protein stability remains a critical issue in the field of biotechnology due to increasing applications and escalating demands of proteins in various industries as biocatalysts, analytical tools, therapeutic agents, clinical diagnostic materials, etc. [1–3]. Proteins are relatively unstable and progressively loose their functionality and native conformation under in vitro conditions such as extreme temperature, pH, pressure as well as in presence of various chemicals and solvents. Such environmental conditions are frequently met in the biotechnology industry and call for further research in order to achieve greater storage and operational stability of proteins including increased shelf life and functionality under these conditions [1].

Although a number of strategies have been demonstrated for increasing protein stability, none of them is proved successful as a general approach for commercialization. These strategies include protein engineering, chemical modification and site-directed mutagenesis [1,4]. Naturally occurring small organic molecules present in the organisms, have shown greater potential to provide significant stabilization to proteins. These small organic molecules such as sugars, polyols, salts, amino acids and their derivatives are collectively termed as osmolytes. Most of the osmolytes have been found compatible with most of the macromolecules in biological systems, hence do not affect the protein functionality or biological activity [2,5,6]. Recently, osmolytes have also been recognized as chemical chaperones due to their protein structure stabilizing ability as well as restoring the folding of the misfolded proteins in biological systems [2]. Exploitation of the above characteristics of osmolytes in stabilizing proteins' structures has given the birth of another phenomenon, known as solvent engineering [7]. Such a strategy has been found promising over to other strategies, particularly in its use for therapeutic agents in treatment of protein misfolding diseases and biocatalysts in the food industry [1,2].

Honey has been used in traditional medicine and as a food supplement since ancient civilization due to its high medicinal and nutritional values. Recent researches have concluded antimicrobial, antibacterial and wound healing properties of honey, which have allowed the use of honey in the treatment of some gastrointestinal, respiratory and ophthalmic disorders and as a topical agent in wound healing treatment [8]. Honey is a mixture of compounds with high-carbohydrate content and rich diversity of minor constituents such as minerals, amino acids, proteins and vitamins. Major component of the honey is sugar, constituting more than 95% of honey dry weight [8]. Various studies have shown that sugars can act as effective osmolytes in increasing protein stability especially, thermal-stability [3,9–17]. Sugars have been shown to provide stabilization to proteins under various stresses such as dehydration, variable pH, freezing, high salinity and in presence of chemical denaturants [1,3,18]. The stabilization mechanism of sugars

Abbreviations: ANS, 1-anilinonaphthalene-8-sulfonate; BSA, bovine serum albumin; CD, circular dichroism; GdnHCl, guanidine hydrochloride; MRE, mean residue ellipticity; SHSC, simulated honey sugar cocktail; Trp, tryptophan; Tyr, tyrosine.

* Corresponding author. Tel.: +60 3 7967 7118; fax: +60 3 7967 4178.
E-mail address: saadtayyab2004@yahoo.com (S. Tayyab).

1359-5113/$ – see front matter © 2012 Elsevier Ltd. All rights reserved.
http://dx.doi.org/10.1016/j.procbio.2012.06.028

cannot be generalized due to the failure of hypotheses/mechanisms to explain the stabilizing phenomenon in some cases [1,19]. In general, protein stability depends on the fine balance between the favorable and unfavorable interactions that maintain its native structure. Thus, sugars seem to stabilize the protein molecule by maintaining these favorable interactions even under stressed environment [3,20].

Irrespective of the mechanism involved, honey may be proved as a potential natural protein stabilizer due to the presence of high sugar content in it. In order to explore the stabilizing potential of honey, it is necessary that honey should be made free from any protein or peptide that could interfere with the experimental procedure as well as data analysis. Hence, simulated honey sugar cocktail (SHSC) was formulated according to the same sugar composition as that found in honey and protein denaturation studies were made using a model protein, bovine serum albumin (BSA) both in the absence and presence of increasing SHSC concentrations. This paper describes the protein stabilizing potential of SHSC using various spectroscopic techniques.

2. Materials and methods

2.1. Materials

Bovine serum albumin (BSA), essentially fatty acid free, type A-6003, urea ultrapure, type U-0631, guanidine hydrochloride (GdnHCl), type G-4505, 1-anilinonaphthalene-8-sulfonate (ANS), type A-3125, D (−) fructose, type F-0127, D (+) trehalose dihydrate, type T-5251 and D (+) glucose, type G-8270 were obtained from Sigma–Aldrich Inc., USA. Sucrose, type SU250-00 and maltose, type 3580-00 were supplied by SYSTERM®, Malaysia and R&M Chemicals, USA respectively. All other reagents used were of analytical grade purity.

2.2. Analytical procedures

Protein concentration was determined spectrophotometrically on a Shimadzu double-beam spectrophotometer; model UV-2450, using a specific absorption coefficient, $\epsilon^{1\%}_{1\ cm}$ of 0.667 at 279 nm [21].

ANS concentration was determined using a molar extinction coefficient, ϵ_m of 5000 M^{-1} cm^{-1} at 350 nm.

Concentrations of stock denaturant (urea and GdnHCl) solutions were determined following the method described by Pace and Scholtz [22].

2.3. Circular dichroism spectroscopy

Jasco spectropolarimeter, model J-815 equipped with a microcomputer was used for circular dichroism (CD) measurements. The instrument was calibrated with d-(+)-camphorsulphonic acid. All CD measurements were performed at 25 °C (unless otherwise stated) using a thermostatically controlled cell holder attached to a water bath with an accuracy of ±0.1 °C. CD spectra were collected with a scan speed of 100 nm min^{-1} and a response time of 1 s. Each spectrum was collected with an average of four scans. Far-UV CD spectra were recorded with a protein concentration of 2.0 μM using a 1 mm path length cell while near-UV CD spectra were measured at a protein concentration of 20 μM with a 10 mm path length cell. The results are expressed as mean residue ellipticity (MRE) in deg cm^2 $dmol^{-1}$ which is defined as:

$$\mathrm{MRE} = \frac{\theta_{obs} \times \mathrm{MRW}}{10 \times l \times C} \quad (1)$$

where θ_{obs} is the CD in millidegree, MRW is mean residue weight (molecular weight of protein, 66,700 divided by total number of amino acids, 582), l is the path length of the cell and C is the protein concentration in mg/ml [23]. Helical content was calculated from the MRE values at 222 nm using the following equation [24]:

$$\%\alpha\text{-helix} = \left[\frac{\mathrm{MRE}_{222} - 2340}{30,300}\right] \times 100 \quad (2)$$

2.4. Fluorescence spectroscopy

Fluorescence measurements were performed on a Hitachi fluorescence spectrophotometer, model F-2500. Fluorescence spectra were recorded at 2.0 μM protein concentration with a 1 cm path length cell. Excitation and emission slits were fixed at 10 nm each. Intrinsic fluorescence was measured by exciting the protein solution at 280 nm and emission spectra were recorded in the wavelength range, 300–400 nm.

In ANS binding studies, the fluorescence spectra were obtained using a protein concentration of 0.2 μM. The emission spectra were recorded in the wavelength range, 400–600 nm upon excitation at 380 nm. Appropriate blank values were subtracted from the fluorescence spectra at each wavelength in order to obtain the net fluorescence caused by the dye absorption.

Three-dimensional (3-D) fluorescence spectra were obtained on a Jasco spectrofluorometer; model FP-6500 using a 1 cm path length cell with a protein concentration of 2.0 μM at 25 °C. The emission wavelength was recorded between 220 nm and 500 nm while the excitation wavelength scan range was 220–350 nm with an increment of 10 nm. The number of scanning curves was 14 and both the excitation and emission slits were set at 10 nm each.

Table 1
Sugar composition in honey and simulated honey sugar cocktail.

Sugar	Percentage content	
	Honey[a] (w/v)	20% (w/v) SHSC[b] (w/v)
Fructose	51.6	10.32
Glucose	46.59	9.32
Sucrose	0.27	0.05
Maltose and trehalose (1:1)	1.26	0.25
Melibiose and other sugars	0.28	–

[a] Adapted from Rybak-Chmielewska and Szczesna [25].
[b] Weight of sugar in gram per 100 ml of 60 mM sodium phosphate buffer, pH 7.4.

2.5. UV difference spectroscopy

Light absorption measurements were made on a Shimadzu double-beam spectrophotometer; model UV-2450 at 25 °C using quartz cuvettes of 1 cm path length. Absorption spectra of protein solution both in the absence and presence of different urea concentrations were recorded in the wavelength range, 250–300 nm against their respective blanks and the difference spectral change was obtained by subtracting the absorbance values of native protein from the absorbance values of the protein in different urea concentrations at each wavelength. Values of absorbance difference were transformed into molar difference extinction coefficient (ϵ) and plotted against wavelength.

2.6. Preparation of simulated honey sugar cocktail

Stock solution [20% (w/v)] of simulated honey sugar cocktail (SHSC) was prepared by dissolving 103.2 g fructose, 93.2 g glucose, 0.5 g sucrose and 1.25 g each of maltose and trehalose in 60 mM sodium phosphate buffer, pH 7.4 in a total volume of 1000 ml. Preparation of 20% (w/v) SHSC solution in the buffer did not significantly affect the pH of the buffer as the change was 0.1 pH unit. Stock SHSC solution was diluted with buffer in a ratio of 1:1 and 1:1.5 to get the final SHSC concentrations as 10% and 8% (w/v), respectively. The sugars' concentrations required in the preparation of different SHSC concentrations corresponded to the sugar composition of the honey as shown in Table 1 [25]. Stock solutions of protein and denaturants (urea and GdnHCl) were prepared in different SHSC solutions as desired in the experiments.

2.7. Denaturation experiments

Stock solutions of protein (200 μM) and denaturants (10.9 M urea and 7 M GdnHCl) were prepared in 60 mM sodium phosphate buffer, pH 7.4 both in the absence and presence of the desired SHSC concentrations [8%, 10% and 20% (w/v)]. Stock protein solutions were diluted to 4 and 8 times with buffer for getting the desired protein concentration needed for far-UV CD, intrinsic fluorescence and ANS fluorescence experiments. For denaturation experiments, different volumes of the buffer (with or without desired SHSC concentrations) were added first to tubes containing a fixed volume of stock protein solution (final concentration = 2.0 μM for far-UV CD and fluorescence measurements; 20 μM for near-UV CD and UV difference spectral measurements and 0.2 μM for ANS binding studies), followed by the addition of different volumes of the stock urea or GdnHCl solutions to obtain the desired concentration of urea or GdnHCl. The final volume of the solution mixture was 5 ml, which was incubated for 12 h at 25 °C before spectral measurements. The denaturation data obtained by different techniques were transformed into the fraction denatured, F_D, using the equation:

$$F_D = \frac{Y - Y_N}{Y_D - Y_N} \quad (3)$$

where different terms have their usual significance [26]. Values of Y_N and Y_D were obtained by linear extrapolation of pre- and post-transition zones of the denaturation curve. The mid-point (C_m value) of the denaturation curve (F_D curve) was determined from the *X*-axis value (urea concentration) at which the *Y*-axis value (F_D) is 0.5. Alternatively, C_m values were also obtained following the procedure described elsewhere [27].

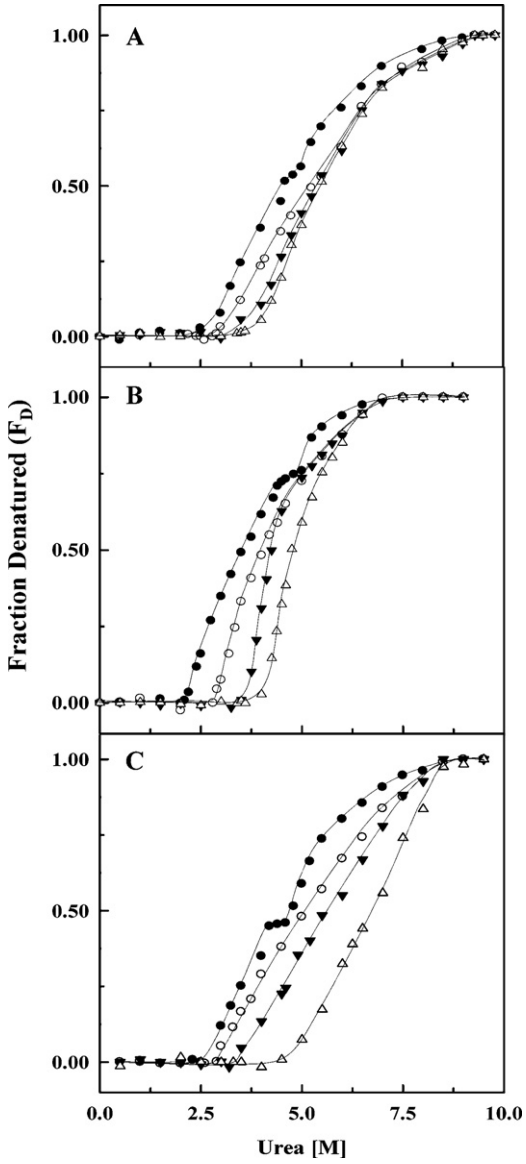

Fig. 1. Normalized transition curves for urea-induced denaturation of BSA as monitored by (A) MRE at 222 nm, (B) intrinsic fluorescence at 341 nm upon excitation at 280 nm and (C) molar extinction coefficient at 288 nm, at pH 7.4 and 25 °C both in the absence (●) and presence of 8% (○), 10% (▼), and 20% (△) (w/v) SHSC.

2.8. Thermal denaturation

Thermal denaturation studies were carried out on a Jasco spectropolarimeter, model J-815 equipped with a peltier type temperature controller (PTC-423S/15). Far UV-CD spectra of the protein solution (2.0 μM) both in the absence and presence of 20% (w/v) SHSC were recorded in the temperature range, 25–100 °C, after equilibrating the protein sample at the desired temperature for 6 min. CD values were transformed into MRE in deg cm^2 dmol^{-1} as described above.

3. Results and discussion

Fig. 1A and B shows the urea-induced denaturation of BSA both in the absence and presence of increasing SHSC concentrations as monitored by $MRE_{222\,nm}$ and intrinsic fluorescence measurements at 341 nm upon excitation at 280 nm. As can be seen from these figures, urea-induced denaturation of BSA was characterized by a two-step, three-state transition, from native (N) state to denatured state (D) via a stable intermediate (I) state which accumulated around ~4.5–5.0 M urea. The first transition (N ⇌ I) started at ~2.0 M urea and completed at ~4.6 M/4.5 M urea whereas the second transition, showing the transformation from the intermediate (I) state to the denatured (D) state (I ⇌ D) started at ~5.0 M urea and sloped off at ~9.3 M and ~8.0 M urea when monitored by $MRE_{222\,nm}$ and intrinsic fluorescence measurements, respectively. These results were in agreement with previous reports on urea-induced denaturation of serum albumin [21,28,29]. Involvement of domain III in the formation of intermediate state during urea denaturation has been suggested [21,28].

Presence of increasing concentrations [8–20% (w/v)] of SHSC in the incubation mixture significantly affected the transition both in terms of the nature and origin. Values of start-, mid- and end-points of the transition of urea-induced denaturation of BSA in the absence and presence of different SHSC concentrations as monitored by different spectroscopic probes are given in Table 2. The transition followed a single-step transition without the detection of intermediate state in the presence of 8–20% (w/v) SHSC (Fig. 1A and B). Furthermore, the transition was also shifted towards higher urea concentration, being positively correlated with SHSC concentrations. In other words, the shift in the transition towards higher urea concentration was more pronounced with 20% (w/v) SHSC compared to that obtained in presence of 8% (w/v) SHSC concentration. More evidently, start- and mid-points of the transition curve increased from 2.8 M and 5.3 M (in presence of 8%, w/v, SHSC) to 3.6 M and 5.5 M urea concentrations (in presence of 20%, w/v, SHSC), respectively as followed by $MRE_{222\,nm}$ measurements (Fig. 1A and Table 2). Similar shift in the start- and mid-points of denaturation were observed in presence of different SHSC concentrations as studied with intrinsic fluorescence measurements (Fig. 1B and Table 2).

Fig. 1C shows urea-induced denaturation of BSA as followed by UV difference spectral measurements both in the absence and presence of increasing SHSC concentrations. These transition curves were qualitatively similar to those obtained with $MRE_{222\,nm}$ and intrinsic fluorescence measurements as shown in Fig. 1A and B. However, quantitative differences were noticed in the value of start-, mid- and end-points of transition (Table 2), in which, the start- and end-points of the transition were ~2.5 M and ~8.5 M urea concentration, respectively, intermediate was accumulated around 4.2–4.6 M urea concentration in native BSA. Earlier report on urea denaturation of BSA has also shown similar characteristics of the transition curve as studied by UV difference spectroscopy [28]. The transition curves obtained in the presence of different SHSC concentrations were characterized by the absence of intermediate state and the late transition when compared to native BSA (Fig. 1C and Table 2). These characteristics were similar to those obtained with $MRE_{222\,nm}$ and intrinsic fluorescence measurements with slight variation in the values of start-, mid- and end-points of the transition. Similar C_m values were obtained when determined from ΔG_D (free energy change of denaturation) versus denaturant concentration curves (Table 2). Since urea concentration range for the denaturation transition was found different with different probes, variation in the mid-point values (C_m values) is expected. In several earlier reports, such type of variation has been shown [28–32]. Both shift in the transition curve towards higher urea concentration and abolishment of intermediate state observed in the presence of different SHSC concentrations using different probes indicated stabilization of the protein by SHSC. In view of the involvement of domain III in the intermediate formation, SHSC seems to stabilize this domain, leading to abolishment of intermediate state in the urea denaturation. Previous reports on urea denaturation of BSA in the presence of fatty acids and salts have also shown a single-step transition with the abolishment of the intermediate state [28,30].

In order to further investigate the stabilizing potential of SHSC on BSA, 4.6 M urea-denatured BSA (representing the intermediate state) was equilibrated with 20% (w/v) SHSC and its properties were studied using far-UV and near-UV CD spectra, UV difference

Table 2
Characteristics of urea denaturation of BSA in the absence and presence of different SHSC concentrations as monitored by different probes.

Experimental probe	Protein sample	Urea-induced transition				Transition pattern
		Start-point [M]	Mid-point (C_m) [M]		End-point [M]	
			(a)	(b)		
MRE at 222 nm	Native BSA					
	• First transition	2.0	3.6	3.5	4.6	Two-step, three-state
	• Second transition	5.0	6.1	5.9	9.3	
	BSA + 8 % (w/v) SHSC	2.8	5.3	5.3	9.3	Single-step, two-state
	BSA + 10 % (w/v) SHSC	3.0	5.4	5.4	9.3	
	BSA + 20 % (w/v) SHSC	3.6	5.5	5.6	9.3	
Intrinsic fluorescence at 341 nm	Native BSA					
	• First transition	2.0	3.1	3.1	4.5	Two-step, three-state
	• Second transition	5.0	5.1	5.2	8.0	
	BSA + 8 % (w/v) SHSC	2.8	3.7	4.0	8.0	Single-step, two-state
	BSA + 10 % (w/v) SHSC	3.25	4.3	4.3	8.0	
	BSA + 20 % (w/v) SHSC	3.6	4.7	4.8	8.0	
Molar difference extinction coefficient at 288 nm	Native BSA					
	• First transition	2.5	3.4	3.4	4.2	Two-step, three-state
	• Second transition	4.6	5.4	5.4	8.5	
	BSA + 8 % (w/v) SHSC	2.9	5.0	5.1	8.5	Single-step, two-state
	BSA + 10 % (w/v) SHSC	3.2	5.5	5.6	8.5	
	BSA + 20 % (w/v) SHSC	4.0	6.6	6.7	8.5	

[a] From F_D curves.
[b] From ΔG_D curves [27].

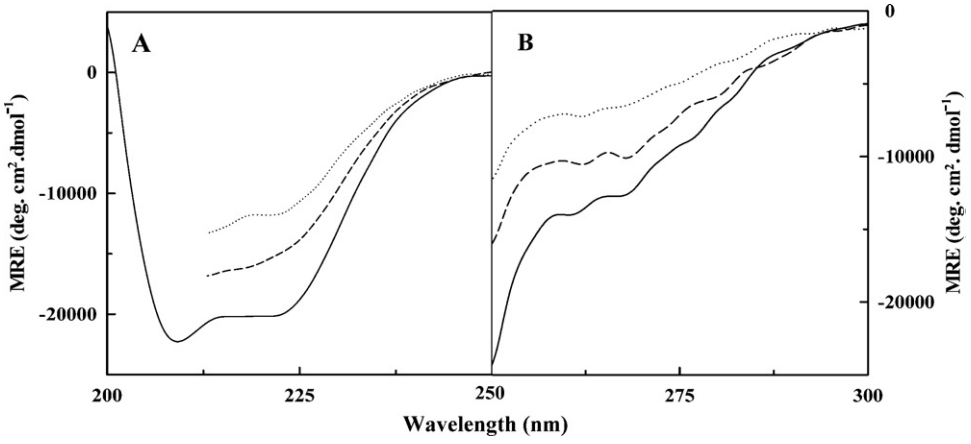

Fig. 2. Far-UV (A) and near-UV (B) CD spectra of native BSA (—) and 4.6 M urea-denatured BSA both in the absence (. . .) and presence (– – –) of 20% (w/v) SHSC at pH 7.4.

Table 3
Spectral characteristics of BSA under various experimental conditions as monitored by different probes.

Spectral characteristics	Native BSA	4.6 M urea-denatured BSA	4.6 M urea-denatured BSA + 20% (w/v) SHSC
MRE at 222 nm (deg cm^2 dmol^{-1})	−20127.1	−11769.4	−15116.6
α-Helical content[a]	~58%	~31%	~42%
MRE at 262 nm (deg cm^2 dmol^{-1})	−13504.30	−7214.97	−10510.70
MRE at 268 nm (deg cm^2 dmol^{-1})	−12601.34	−6481.79	−10095.55
Molar difference extinction coefficient at 288 nm ($\times 10^{-3}$)	–	−2.8	−0.9
ANS fluorescence intensity at 469 nm	273.26	33.62	112.78

[a] Calculated by the method of Chen et al. [24]

spectra, three-dimensional fluorescence spectra as well as ANS binding. Fig. 2A and B shows the effect of 20% (w/v) SHSC on the far-UV and near-UV CD spectra of partially denatured BSA, obtained in 4.6 M urea at pH 7.4. Far-UV and near-UV CD spectra of native BSA at pH 7.4 are also included for comparison. Far-UV CD spectra are generally used to probe secondary structures in proteins [33–35]. The far-UV CD spectrum of native BSA was characterized by the presence of two minima at 208 nm and 222 nm, characteristics of α-helical structures in proteins [33]. The spectra of partially denatured BSA at 4.6 M urea in the absence and presence of 20% (w/v) SHSC retained the characteristic features of α-helical structure, showing the minima at 222 nm. However, the magnitude of $MRE_{222\,nm}$ was found higher (∼28%) in presence of 20% (w/v) SHSC compared to the one obtained in its absence, but lower (∼25%) than $MRE_{222\,nm}$ of native BSA (Fig. 2A and Table 3). It should be noted that far-UV CD spectra of partially denatured BSA at 4.6 M urea both in the absence and presence of 20% (w/v) SHSC could not be obtained below 213 nm due to high signal to noise ratio. A more quantitative analysis of far-UV CD spectra was made by calculating the percentage α-helical content using the method of Chen et al. [24] and the values of α-helical content are given in Table 3. As can be seen from the table, α-helical content decreased from ∼58% (for native BSA) to ∼31% in the presence of 4.6 M urea, showing a decrease of ∼27%. Similar decrease in the α-helical content in urea-induced intermediate of serum albumin has also been reported earlier [29]. Interestingly, addition of 20% (w/v) SHSC in the incubation mixture stabilized the native protein conformation by inducing ∼11% increase in the α-helical content at the same urea concentration (Table 3). Although this stabilizing effect was significant but was not enough to retain the native protein structure within this urea concentration range. In view of the involvement of domain III in the intermediate formation during urea denaturation [21,28], it seems that 20% (w/v) SHSC stabilized this domain to a significant extent during urea denaturation. To check the structural integrity of BSA in presence of 20% (w/v) SHSC, we determined far-UV CD spectra of BSA both in the absence and presence of 20% (w/v) SHSC and the obtained overlapping CD spectra (figure omitted for brevity) suggested that the structural integrity of BSA was retained in presence of SHSC.

The stabilizing effect of 20% (w/v) SHSC on the tertiary structure of partially denatured BSA can be seen from Fig. 2B, showing near-UV CD spectra of 4.6 M urea-denatured BSA in the absence and presence of 20% (w/v) SHSC along with native BSA. Presence of two troughs at 262 nm and 268 nm along with two shoulders at 275 nm and 292 nm characterized the near-UV CD spectrum of native BSA. Previous studies have also shown the presence of these spectral features in the near-UV CD spectrum of BSA [33,35]. The origin of these spectral features has been ascribed to the presence of disulphide bonds and aromatic chromophores [36]. Decrease in the MRE values at 262 nm and 268 nm, observed in the near-UV CD spectrum of partially denatured BSA indicated significant loss in the tertiary structure of the protein. Significant stabilization of the native protein structure by 20% (w/v) SHSC was evident from the near-UV CD spectrum of partially denatured BSA, obtained in the presence of 20% (w/v) SHSC (Fig. 2B), where the MRE values at 262 nm and 268 nm were found to be significantly higher (∼46% and ∼56%, respectively) than those of 4.6 M urea-denatured BSA (Table 3). These results were similar to those obtained with far-UV CD spectra, suggesting stabilizing potential of 20% (w/v) SHSC against urea denaturation of BSA.

Fig. 3 shows UV difference spectra of partially denatured BSA at 4.6 M urea both in the absence and presence of 20% (w/v) SHSC. The UV difference spectrum of partially denatured BSA against native BSA was characterized by the presence of a pronounced trough at 288 nm along with a shoulder at 280 nm. Similar spectral features in the UV difference spectrum of urea-denatured BSA

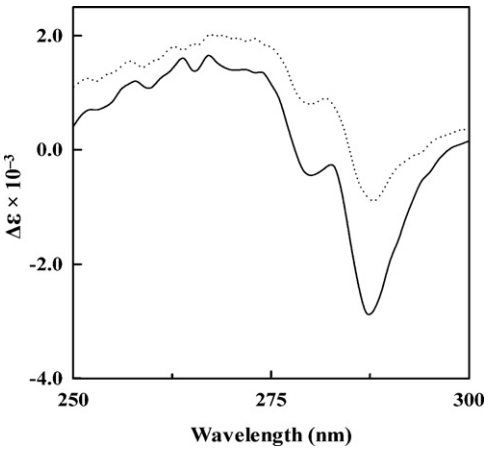

Fig. 3. UV difference spectra of 4.6 M urea-denatured BSA both in the absence (—) and presence (. . .) of 20% (w/v) SHSC at pH 7.4.

have been reported earlier [28]. These spectral features of the UV difference spectrum were indicative of the perturbation of environment around tyrosine (Tyr) residues [37]. A slight bulging near 292–295 nm in the UV difference spectrum of 4.6 M urea-denatured BSA both in the absence and presence of 20% (w/v) SHSC was suggestive of the environmental fluctuations around tryptophan residues (Trp 134 and Trp 212) of BSA at 4.6 M urea concentration [28]. Presence of 20% (w/v) SHSC offered significant stabilization to BSA against urea denaturation as reflected from the marked decrease in the magnitude of UV difference spectrum of partially denatured BSA in presence of 20% (w/v) SHSC. The significant decrease in molar difference extinction coefficient at 288 nm (Fig. 3 and Table 3) suggested stabilization of domains I and II of BSA in presence 20% (w/v) SHSC, as most of the Tyr residues are mainly located in domains IB and IIB of BSA [38].

ANS binding was used to investigate the exposure of hydrophobic regions in BSA under different experimental conditions. Fig. 4 shows ANS fluorescence spectra of native BSA and 4.6 M urea-denatured BSA both in the absence and presence of 20% (w/v) SHSC. ANS in free form shows little fluorescence and produces a marked increase in the fluorescence upon binding to hydrophobic regions in proteins [34]. Native BSA produced a significant ANS fluorescence spectrum in the wavelength range, 400–600 nm, which was suggestive of the presence of the significant hydrophobic surfaces in the native protein. These results were in accordance to a

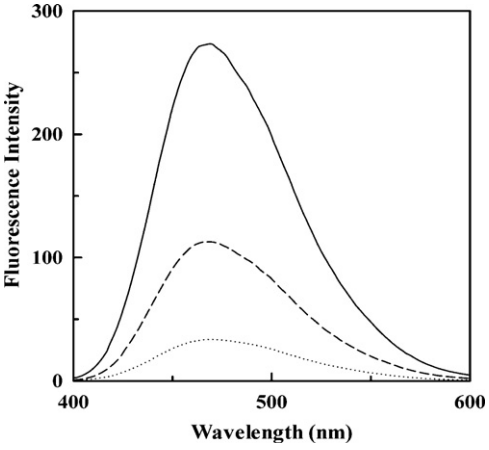

Fig. 4. ANS fluorescence spectra in presence of native BSA (—) and 4.6 M urea-denatured BSA both in the absence (. . .) and presence (– –) of 20% (w/v) SHSC at pH 7.4.

previous report showing ~10 ANS binding sites available in the native BSA [39]. There was a remarkable decrease (~88%) in ANS fluorescence in presence of 4.6 M urea as shown by ANS fluorescence spectrum of partially denatured BSA (Fig. 4 and Table 3). Although more hydrophobic residues would have been exposed in 4.6 M urea-denatured BSA, nevertheless, the binding of ANS to BSA required the organized hydrophobic clusters instead of individual hydrophobic residues [40], which would have been disorganized in presence of 4.6 M urea. Additionally, presence of urea would have disrupted the hydrophobic interactions involved in the binding of ANS to these exposed hydrophobic regions [40]. In view of the above, decrease in the ANS fluorescence of BSA in presence of 4.6 M urea was not astonishing. Similar observations on the decrease in ANS fluorescence of other proteins in presence of urea have been reported earlier [34,40]. Stabilizing effect of 20% (w/v) SHSC on BSA against urea denaturation can be clearly seen from the ANS fluorescence spectrum of 4.6 M urea-denatured BSA in presence of 20% (w/v) SHSC. A significant recovery in ANS fluorescence exhibited by partially denatured BSA in presence of 20% (w/v) SHSC [3.35-fold higher than that observed in the absence of 20% (w/v) SHSC] indicated significant retention of native-like structure with more hydrophobic clusters in this preparation (Fig. 4 and Table 3). These results suggested that the conformation of 4.6 M urea-denatured BSA in presence of 20% (w/v) SHSC was more conserved.

Three-dimensional fluorescence was used as an additional probe to study conformational changes in BSA at 4.6 M urea both in the absence and presence of 20% (w/v) SHSC [27]. The 3-D fluorescence spectra and contour maps of native BSA and partially denatured BSA at 4.6 M urea both in the absence and presence of 20% (w/v) SHSC are shown in Fig. 5 and corresponding characteristic parameters are listed in Table 4. As can be seen from Fig. 5, peaks '*a*' and '*b*' represented Rayleigh scattering peak ($\lambda_{em} = \lambda_{ex}$) and the second-order scattering peak ($\lambda_{em} = 2\lambda_{ex}$), respectively. Two additional peaks, namely, peaks 1 and 2, representing fluorescence peaks were also observed. The peak 1 (λ_{ex} = 280 nm) also known as the primary fluorescence peak mainly revealed the spectral behavior of Tyr and Trp residues in the three-dimensional structure of the protein as excitation of BSA at 280 nm leads to the intrinsic fluorescence due to Tyr and Trp residues. The emission maximum and the fluorescence intensity of the peak characterize the polarity of the fluorophores' microenvironment [41]. Presence of 4.6 M urea significantly decreased the fluorescence intensity of peak 1 compared to that obtained with native BSA in a ratio of 0.67:1.00 (Fig. 5 and Table 4). Decrease in the fluorescence intensity of peak 1 may result from the quenching due to the loss in the tertiary structure leading to the unfolding of domain III of BSA whereas rearrangement of domains I and II may account for a 5 nm blue shift [21]. Interestingly, there was a significant recovery in the fluorescence intensity of 4.6 M urea-denatured BSA in presence of 20% (w/v) SHSC as the ratio of the fluorescence intensity of 4.6 M urea-denatured BSA to that of native BSA, in presence of 20% (w/v) SHSC increased to 0.88:1.00. Furthermore, increase in the blue shift (9 nm) observed with 4.6 M urea-denatured BSA in presence of 20% (w/v) SHSC may be ascribed to a greater internalization of Trp residues as compared to the shift noticed in the absence of 20% (w/v) SHSC. The stabilizing effect of 20% (w/v) SHSC on the tertiary structure of protein molecule as shown by 3-D fluorescence results was in agreement with the near-UV CD spectral results, shown in Fig. 2B.

Occurrence of peak 2 (λ_{ex} = 230 nm) in the 3-D spectra and the contour maps of BSA indicated the fluorescence characteristics of the polypeptide backbone correlating to the secondary structure of the protein [41]. Similar to the observation noticed with peak 1, the fluorescence intensity of peak 2 of BSA also showed a marked reduction (in a ratio of 0.42:1.00) in the presence of 4.6 M urea. Such a drastic decrease in the fluorescence intensity was suggestive of the significant loss in the secondary structure of 4.6 M urea-denatured BSA. This was in line with our far-UV CD spectral results, showing a significant reduction in the α-helical content in 4.6 M urea-denatured BSA. There was a significant recovery in the fluorescence intensity of peak 2 of 4.6 M urea-denatured BSA compared to native BSA in the presence of 20% (w/v) SHSC (in a ratio of 0.53:1.00), suggesting stabilization of secondary structures in presence of 20% (w/v) SHSC. These results were in accordance with our far-UV CD spectral results.

The protein stabilizing potential of SHSC was further evaluated using thermal- and GdnHCl denaturation studies of BSA in the absence and presence of 20% (w/v) SHSC. Thermal denaturation profiles of BSA as monitored by $MRE_{222\,nm}$ both in the absence and presence of 20% (w/v) SHSC are shown in Fig. 6A. As can be seen from the figure, $MRE_{222\,nm}$ value of native BSA decreased on increasing the temperature, indicative of structural derangement of native BSA. However, the decrease was found slower within the temperature range, 25–45 °C, became more pronounced between 45 and 80 °C and slowed down above 85 °C. Increase in enthalpy change within 45–80 °C was primarily responsible for observed structural disorganization [42]. Similar helical structural changes within this temperature range have been shown earlier [43,44]. Thermal denaturation of BSA in the presence of 20% (w/v) SHSC followed the similar pattern up to 45 °C as that observed in the absence of 20% (w/v) SHSC. In contrast, it showed extension in the slow phase up to 60 °C beyond which a sharp decrease in $MRE_{222\,nm}$ was noticed up to 100 °C in presence of 20% (w/v) SHSC. In other words, thermal denaturation curve of BSA in the presence of 20% (w/v) SHSC was shifted towards higher temperature range, indicating thermal stabilization of BSA by the SHSC. At any given temperature within the temperature range, 60–100 °C, values of MRE_{222nm}, representing α-helical content in BSA, were found higher in presence of 20% (w/v) SHSC compared to those obtained in its absence.

Fig. 6B shows far-UV CD spectra of BSA at 25 °C as well as 65 °C both in the absence and presence of 20% (w/v) SHSC. As can be seen from the figure, CD spectrum of BSA at 65 °C showed lesser secondary structural features (~35% α-helix) than those obtained at 25 °C (~60% α-helix), indicative of thermal denaturation (Table 5). However, CD spectra of BSA obtained at 65 °C but in presence of 20% (w/v) SHSC showed significant retention in the secondary structures (~46% α-helix), which was suggestive of protein stabilization by 20% (w/v) SHSC (Table 5). No sign of Maillard reaction in the SHSC-BSA mixture was seen up to 85 °C. However, little Maillard reaction occurred at temperatures above 85 °C. This would not affect the overall conclusion that 20% (w/v) SHSC provided the significant thermal-stabilization to BSA as indicated in Fig. 6A and B within the temperature range, 50–85 °C. Moreover, in a previous study on the thermal denaturation of ribonuclease A in presence of reducing sugars, Poddar et al. [13], have not reported the occurrence of Maillard reaction up to 85 °C.

Fig. 7A shows GdnHCl-induced denaturation of BSA in the absence and presence of 20% (w/v) SHSC as studied by $MRE_{222\,nm}$ measurements. The denaturation of native BSA was characterized by a single-step, two-state transition, which started at ~1.3 M and sloped off at ~5.5 M GdnHCl concentrations. A previous study on denaturation of serum albumin by GdnHCl has shown similar results [29]. The denaturation curve of BSA was shifted towards a higher GdnHCl concentration in the presence of 20% (w/v) SHSC, showing the start- and mid-points of denaturation at ~1.6 M and 2.3 M against ~1.3 M and 1.9 M GdnHCl, respectively, observed in its absence (Table 5). The shift in the whole transition curve was indicative of protein stabilization by 20% (w/v) SHSC. Lesser shift in the GdnHCl denaturation curve compared to urea denaturation curve in the presence of 20% (w/v) SHSC can be attributed to the stronger action of GdnHCl to denature proteins [29]. As supportive evidence, far-UV CD spectra of native and partially denatured BSA at

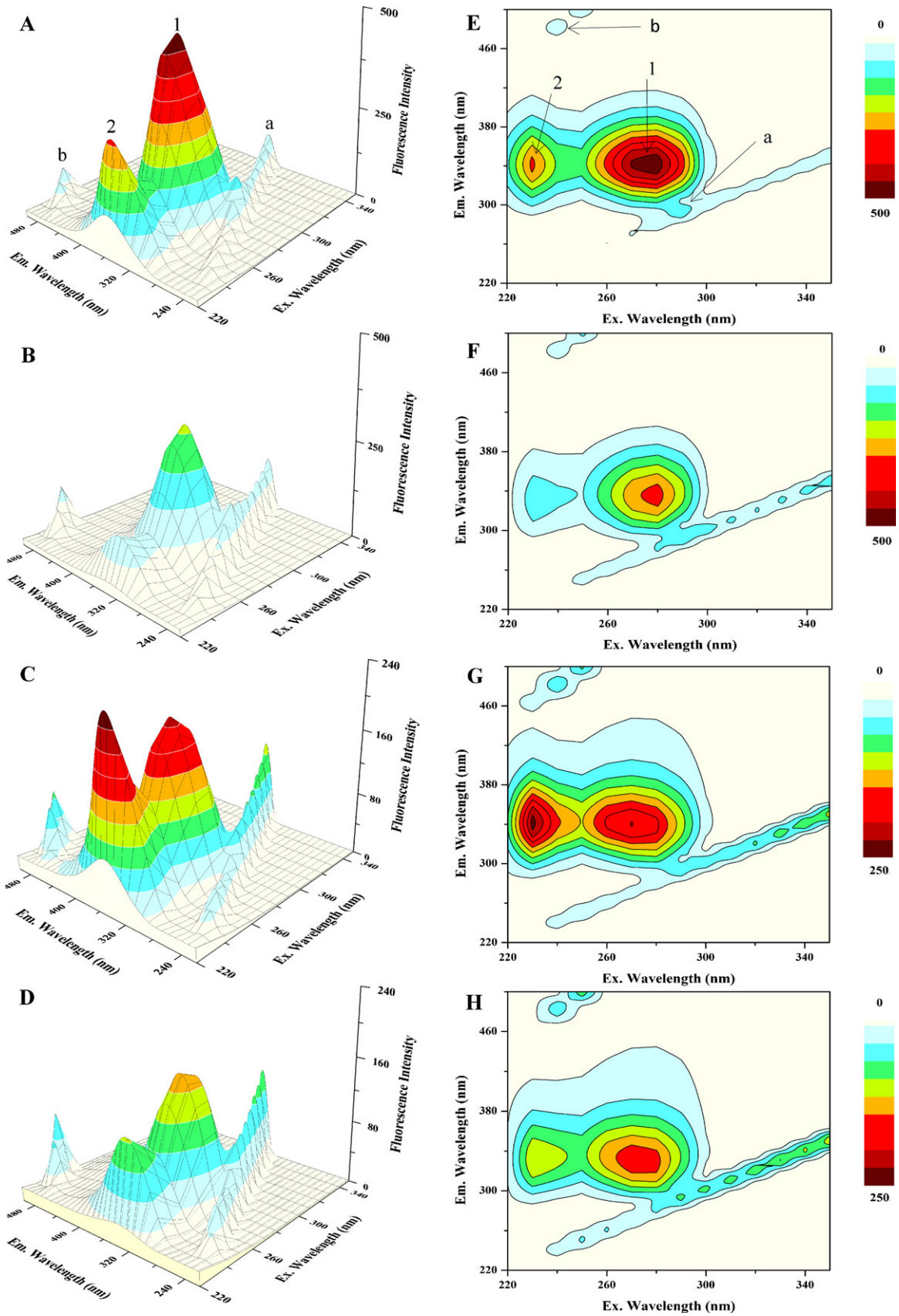

Fig. 5. Three-dimensional fluorescence spectra (A, B, C, D) and corresponding contour maps (E, F, G, H) for native and 4.6 M urea-denatured BSA under various experimental conditions. (A) and (E) for native BSA; (B) and (F) for 4.6 M urea-denatured BSA; (C) and (G) for native BSA in presence of 20% (w/v) SHSC; (D) and (H) for 4.6 M urea-denatured BSA in presence of 20% (w/v) SHSC.

Table 4
Three-dimensional fluorescence spectral characteristics of BSA under various experimental conditions.

Protein sample	Peak	Peak position [$\lambda_{ex}/\lambda_{em}$ (nm/nm)]	Intensity
Native BSA	a	230/230 ⟶ 350/350	17.70 ⟶ 91.83
	b	250/500	85.89
	1	280/341	485.21
	2	230/341	313.72
4.6 M urea-denatured BSA	a	230/230 ⟶ 350/350	16.75 ⟶ 129.79
	b	250/500	114.45
	1	280/336	324.09
	2	230/332	132.18
Native BSA + 20 % (w/v) SHSC	a	230/230 ⟶ 350/350	17.12 ⟶ 108.19
	b	250/500	80.29
	1	280/339	182.12
	2	230/342	233.84
4.6 M urea-denatured BSA + 20 % (w/v) SHSC	a	230/230 ⟶ 350/350	15.40 ⟶ 114.89
	b	250/500	92.48
	1	280/330	160.02
	2	230/332	124.79

1.9 M GdnHCl both in the absence and presence of 20% (w/v) SHSC are shown in Fig. 7B. The far-UV CD spectrum of 1.9 M GdnHCl-denatured BSA in presence of 20% (w/v) SHSC showed a significant shift towards the native spectrum of BSA within the whole wavelength range studied, which indicated the retention of secondary structural characteristics, particularly, α-helical content. Values of $MRE_{222\,nm}$ and respective α-helical content of native and 1.9 M GdnHCl-denatured BSA in the absence and presence of 20% (w/v) SHSC are given in Table 5. As can be clearly seen from the table, α-helical content of 1.9 M GdnHCl-denatured BSA increased from ~25% to ~40% in the presence of 20% (w/v) SHSC.

Many studies have shown the stabilizing potential of sugars (mono-, di- and trisaccharides) on proteins against different denaturing conditions, particularly, thermal denaturation [3,9–17]. Several mechanisms have been proposed in support of sugar-induced protein stabilization [5,7,8,10,16,45,47–53]. However, no single mechanism can be generalized to explain protein stabilization phenomenon in presence of sugars. According to Timasheff

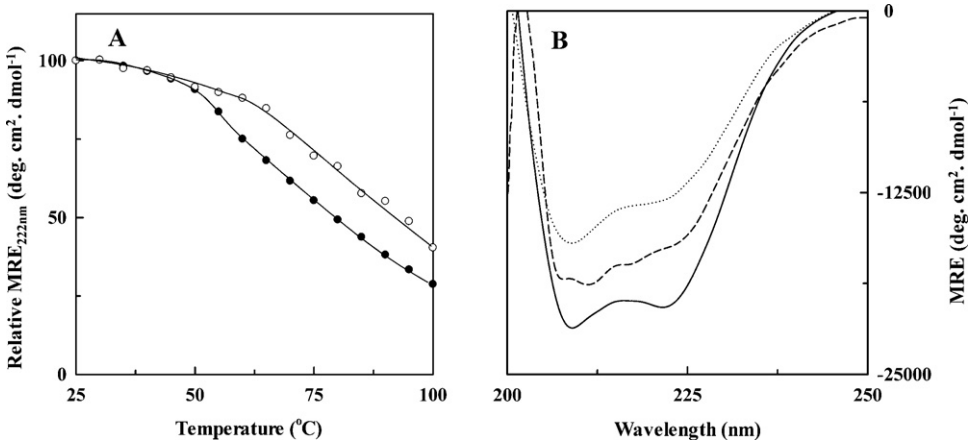

Fig. 6. (A) Thermal denaturation profiles of native BSA at pH 7.4, both in the absence (●) and presence (○) of 20% (w/v) SHSC as followed by $MRE_{222\,nm}$ measurements. (B) Far-UV CD spectra of native BSA at pH 7.4, 25°C (—) and 65°C both in the absence (. . .) and presence (– –) of 20% (w/v) SHSC.

Table 5
Characteristics of GdnHCl- and thermal denaturation of BSA in the absence and presence of 20% (w/v) SHSC as monitored by $MRE_{222\,nm}$ measurements.

Characteristics	BSA	BSA + 20% (w/v) SHSC
GdnHCl denaturation		
– Start-point	1.3 M GdnHCl	1.6 M GdnHCl
– Mid-point	1.9 M GdnHCl	2.3 M GdnHCl
– $MRE_{222\,nm}$ (α-helix)		
• Native	−20,353.7 (∼59%)	−20,227.1 (∼59%)
• 1.9 M GdnHCl-denatured	−9800.1 (∼25%)	−14,423.3 (∼40%)
Thermal denaturation (fast phase)		
– Start-point	45 °C	60 °C
– $MRE_{222\,nm}$ (α-helix)		
• 25 °C	−20,370.6 (∼60%)	−20,244.0 (∼59%)
• 65 °C	−12,972.0 (∼35%)	−16,317.0 (∼46%)

[5,45–49], preferential hydration of proteins is noted to be a common feature in presence of sugars irrespective of the kind of protein and solvent conditions [46]. Preferential hydration of proteins is favored due to stronger interactions between sugar and water molecules compared to those between sugar and protein molecules. This was supported by simulation studies, showing single hydrogen bond formation between sugar and protein molecules while water molecules act as the bridge between sugar and protein molecules [53,54]. Addition of sugars to an aqueous protein solution results in a positive (unfavorable) free energy change in the protein which is assumed to be higher in the denatured state of the protein due to greater surface area [45]. Therefore, in sugar solutions, the equilibrium is supposed to be shifted towards native protein conformation, thus favoring the protein stabilization [5,47]. Besides the interaction between the polar residues on the protein surface and water molecules, residual nonpolar region at the protein surface, preferentially excludes the sugar molecules. Furthermore, steric exclusion may result in a little volume fraction occupied by sugar molecules at the protein surface, thus manifesting preferential hydration [47,49].

In accordance to Timasheff's mechanism, Bolen and Baskakov [50] also suggested the increase in the Gibbs free energy of the protein molecule in presence of sugars. It was suggested that osmolyte-induced stabilization of protein against denaturing conditions mainly arises from the unfavorable (solvophobic) interactions between osmolytes and the polypeptide backbone which is termed as 'osmophobic effect'. The denatured state being more solvophobic towards osmolytes than the native state, increases the Gibbs free energy far greater than its native counterpart [50,51]. In view of the greatly exposed polypeptide backbone in the denatured state of the protein, this osmophobic effect would be more pronounced. Hence, addition of sugars would have favored the native state of the protein due to the displacement of the equilibrium between native and denatured states of the protein towards the native state [50]. Preferential hydration model was also endorsed by a report suggesting no direct interaction between sugar and protein molecules rather sugar molecules concentrate water molecules in the vicinity of protein [56]. High viscosity hypothesis [16] supports the protein stabilization for low water system due to the inhibition of molecular motion and dynamic processes under high viscosity. This inhibition of molecular motion and protein dynamics was also supported by molecular dynamic simulation studies [17].

Smith and co-workers [52] conceived the idea of protein stabilization by sugars through alteration in water structure, which in turn determines the strength of hydrophobic interactions. The presence of sugars in the solvent would have changed the solvent properties in the vicinity of protein molecule, leading to stronger hydrophobic interactions in protein. This change in solvent properties would have been responsible for reducing the hydrogen rupturing potency of surrounding water molecules in the vicinity of protein, thus leading to protein stabilization [53]. Water molecules connect different sugar molecules to each other as well as to the protein surface via hydrogen bonds, forming a water-mediated hydrogen bond network [54,55]. This hydrogen bond network renders the interaction between protein and water molecules less favorable as compared to that in the absence of sugar. In view of the above, water molecules are hindered from penetrating the protein interior and breaking the internal hydrogen bonds [57]. Besides, this network also hindered the water molecules at the protein surface from breaking the surface hydrogen bonds formed between the surface polar residues.

A few reports on the use of co-solute mixtures [13,58], have suggested that the stabilizing effect of the sugar mixtures is an

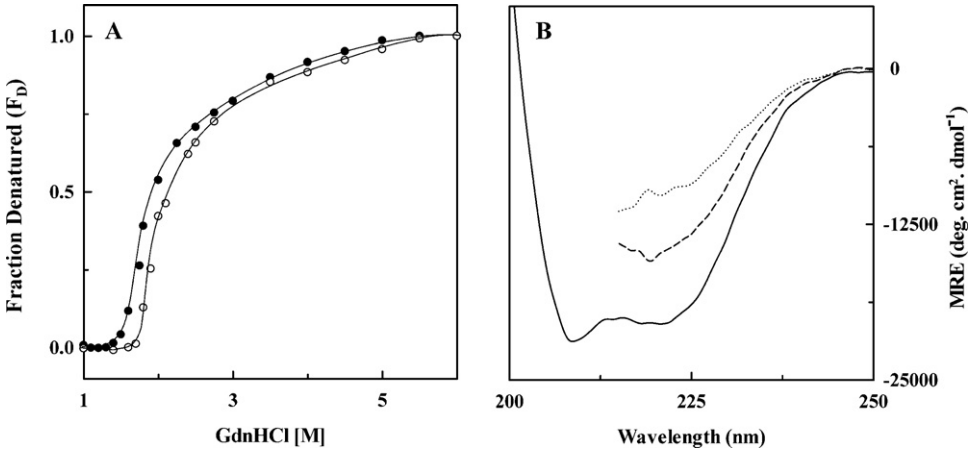

Fig. 7. (A) Normalized transition curves for GdnHCl-induced denaturation of BSA both in the absence (●) and presence (○) of 20% (w/v) SHSC as followed by $MRE_{222\,nm}$ measurements at pH 7.4, 25 °C. (B) Far-UV CD spectra of native BSA (—) and 1.9 M GdnHCl-denatured BSA both in the absence (. . .) and presence (– – –) of 20% (w/v) SHSC.

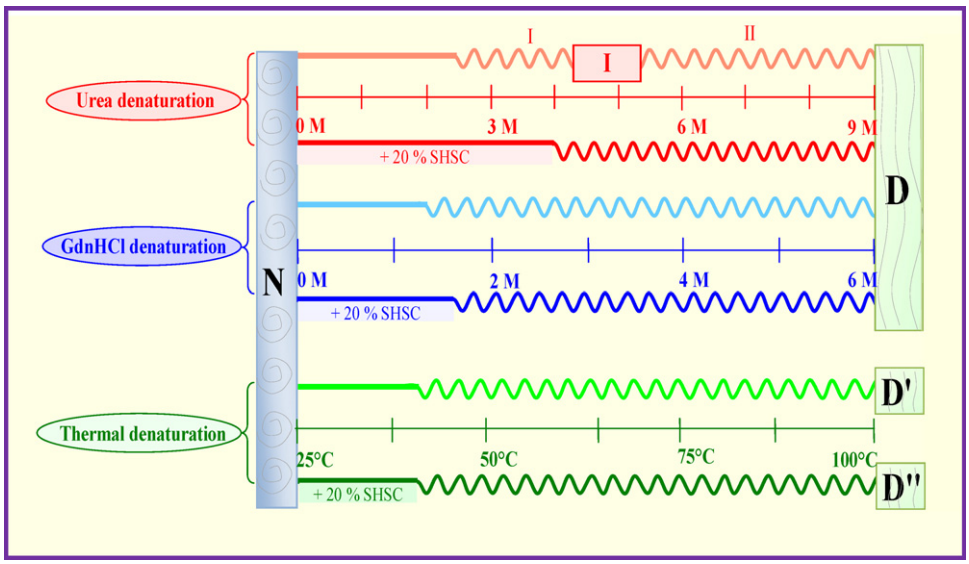

Scheme 1. Scheme showing the stabilization effect of 20% (w/v) SHSC on urea-, GdnHCl- and thermal denaturation of BSA. Symbols N and D refer to native and denatured states of the protein, respectively, whereas D′ and D″ represent heat-denatured states formed upon thermal denaturation of BSA in the absence and presence of 20% (w/v) SHSC, respectively. Solid lines show the native state, whereas the wavy lines demonstrate the denaturation. Lines shown in light color represent denaturation of BSA in the absence of 20% (w/v) SHSC, whereas those in dark color show denaturation in the presence of 20% (w/v) SHSC. (For interpretation of the references to color in this scheme legend, the reader is referred to the web version of the article.)

additive function and equimolar mixtures of different sugars provide better stabilization than the similar molarity of the individual sugars. This implies that SHSC being a sugar mixture would provide greater protein stabilizing effect than the equal concentration of individual sugar components. It may significantly reduce the sugar concentration required in achieving the same extent of stabilization.

Since SHSC represents a mixture of sugars, mainly fructose and glucose, presence of SHSC would have displaced the native state (N) ⇌ denatured state (D) equilibrium of the protein towards the native state through both preferential hydration as well as osmophobic effect as described by Timasheff [45–49] and Bolen [50,51], respectively. According to high viscosity hypothesis [16], SHSC would have also hindered the protein dynamic processes. In view of the above, stabilization of BSA in the presence of SHSC seems to be controlled by thermodynamic forces as well as inhibition of protein dynamic processes, known to promote protein denaturation. Presence of SHSC led to the formation of a different denatured state of the protein. This has been shown in Scheme 1. Several reports have suggested the difference between thermal-denatured state (less denatured with some residual structure) and the complete denatured state, obtained in presence of chemical denaturants such as 9 M urea or 6 M GdnHCl [59–61]. We also noticed different denatured states of BSA obtained in presence of 9 M urea/6 M GdnHCl (D-state) as well as at 100 °C (D'-state) as studied by different spectroscopic probes. Although similar kind of changes were noticed in presence of 20% (w/v) SHSC, the extent of denaturation was found lesser compared to that obtained at 100 °C. In view of this, thermal-denatured state of the protein in presence of 20% (w/v) SHSC (D″-state) seems to be different from the denatured state obtained at 100 °C. In conclusion, SHSC stabilized BSA against urea-, GdnHCl- and thermal denaturation to a significant extent.

Acknowledgments

This work was financially supported by a HIR grant (F000002-21001) sanctioned by the Ministry of Higher Education, Government of Malaysia and the University of Malaya to S.T. YHW is the Research Assistant in this project. We gratefully acknowledge the facilities provided by the Institute of Biological Sciences, Faculty of Science, University of Malaya.

References

[1] Fagain CO. Enzyme stabilization-recent experimental progress. Enzyme Microb Technol 2003;33:137–49.
[2] Arakawa T, Ejima E, Kita Y, Tsumoto K. Small molecule pharmacological chaperones: from thermodynamic stabilization of pharmaceutical drugs. Biochim Biophys Acta 2006;1764:1677–87.
[3] Singh LR, Poddar NK, Dar TA, Rahman S, Kumar R, Ahmad F. Forty years of research on osmolytes-induced protein folding and stability. J Iran Chem Soc 2011;8:1–23.
[4] Campos LA, Garcia-Mira MM, Godoy-Ruiz R, Sanchez-Ruiz JM, Sancho J. Do proteins always benefits from a stability increase? Relevant and residual stabilization in a three-state protein by charge optimization. J Mol Biol 2004;344:223–37.
[5] Arakawa T, Timasheff SN. Stabilization of protein structure by sugars. Biochemistry 1982;21:6536–44.
[6] Anjum F, Rishi V, Ahmad F. Compatibility of osmolytes with Gibbs energy of stabilization of proteins. Biochim Biophys Acta 2000;1476:75–84.
[7] Wangikar PP, Graycar TP, Estell DA, Clark DS, Drodick JS. Protein and solvent engineering of substilisin BPN' in nearly anhydrous organic media. J Am Chem Soc 1993;115:12231–7.
[8] Bogdanov S, Jurendic T, Sieber R, Gallmann P. Honey for nutrition and health: a review. J Am Coll Nutr 2008;27:677–89.
[9] Baier S, McClements DJ. Impact of preferential interaction on thermal stability and gelation of bovine serum albumin in aqueous sucrose solutions. J Agric Food Chem 2001;49:2600–8.
[10] Kaushik JK, Bhat R. Why is trehalose an exceptional protein stabilizer? J Biol Chem 2003;278:26458–65.
[11] Gheibi N, Saboury AA, Haghbeen K, Moosavi-Movahedi AA. The effect of some osmolytes on the activity and stability of mushroom tyrosinase. J Biosci 2006;31:355–62.
[12] Miroliaei M, Ranjbar B, Manesh HN, Nemat-Gorgani M. Thermal denaturation of yeast dehydrogenase and protection of secondary and tertiary structural changes by sugars: CD and fluorescence studies. Enzyme Microb Technol 2007;40:896–901.
[13] Poddar NK, Ansari ZA, Singh RK, Moosavi-Movahedi AA, Ahmad F. Effect of monomeric and oligomeric sugar osmolytes on ΔG_D, the Gibbs energy of stabilization of the protein in different pH values: is the sum effect of monosaccharide individually additive in a mixture? Biophys Chem 2008;138:120–9.
[14] Naika GS, Prakash V, Tiku PK. Effect of cosolvents in the structural stability of endoglucanase from *Aspergillus aculeatus*. J Agric Food Chem 2009;57:10450–6.
[15] Yadav JK, Prakash V. Thermal stability of α-amylase in aqueous cosolvent systems. J Biosci 2009;34:377–87.
[16] Bellavia G, Cottone G, Giuffrida S, Cupane A, Cordone L. Thermal denaturation of myoglobin in water-disaccharide matrixes: relation with the glass transition of the system. J Phys Chem B 2009;113:11543–9.

[17] Bellavia G, Giuffrida S, Cottone G, Cupane A, Cordone L. Protein thermal denaturation and matrix glass transition in different protein–trehalose–water systems. J Phys Chem B 2011;115:6340–6.
[18] Yancey PH. Organic osmolytes as compatible, metabolic and counteracting cytoprotectants in high osmolarity and other stresses. J Exp Biol 2005;208:2819–30.
[19] Lebret A, Bordat P, Affouard F, Descamps M, Migliardo F. How homogenous are the trehalose, maltose, and sucrose water solution? An insight from molecular dynamics stimulations. J Phys Chem B 2005;109:11046–57, and references therein.
[20] Tiwari A, Bhat R. Stabilization of yeast hexokinase A by polyol osmolytes: correlation with the physicochemical properties of aqueous solutions. Biophys Chem 2006;124:90–9.
[21] Tayyab S, Sharma N, Khan MM. Use of domain specific ligands to study urea-induced unfolding of bovine serum albumin. Biochem Biophys Res Commun 2000;277:83–8.
[22] Pace CN, Scholtz JM. Measuring the conformational stability of a protein. In: Creighton TE, editor. Protein structure: a practical approach. Oxford: Oxford University Press; 1997. p. 299–321.
[23] Tan CY, Rahman RNZ, Kadir HA, Tayyab S. Calcium-induced stabilization of α-amylase against guanidine hydrochloride denaturation. Afr J Biotechnol 2010;9:7934–41.
[24] Chen YH, Yang JT, Martinez M. Determination of the secondary structure of proteins by circular dichroism and optical rotatory dispersion. J Biochem 1972;11:4120–31.
[25] Rybak-Chmielewska H, Szczesna T. Composition and properties of polish buckwheat honey. In: Matano T, Vjihara A, editors. Current advances in Buckwheat research. Shinshu: Shinshu University Press; 1995. p. 793–9.
[26] Pace CN. Determination and analysis of urea and guanidine hydrochloride denaturation curves. Methods Enzymol 1986;131:266–80.
[27] Zaroog MS, Tayyab S. Formation of molten globule-like state during acid denaturation of *Aspergillus niger* glucoamylase. Process Biochem 2012;47:775–84.
[28] Ahmad N, Qasim MA. Fatty acid binding to bovine serum albumin prevents formation of intermediate during denaturation. Eur J Biochem 1995;227:563–5.
[29] Muzammil S, Kumar K, Tayyab S. Anion-induced stabilization of human serum albumin prevents the formation of intermediate during urea denaturation. Proteins: Struct Funct Genet 2000;40:29–38.
[30] Tayyab S, Ahmad B, Kumar Y, Khan MM. Salt-induced refolding in different domains of partially folded bovine serum albumin. Int J Biol Macromol 2002;30:17–22.
[31] Khan MY, Agarwal SK, Hangloo S. Urea-induced structural transformations in bovine serum albumin. J Biochem 1987;102:313–7.
[32] Hung HC, Chang GG. Multiple unfolding intermediates of human placental alkaline phosphatase in equilibrium urea denaturation. Biophys J 2001;81:3456–71.
[33] Pelton JT, McLean LR. Spectroscopic methods for analysis of protein secondary structure. Anal Biochem 2000;277:167–76.
[34] Botelho MG, Gralle M, Oliveira CLP, Torriani I. Folding and stability of the extracellular domain of the human amyloid precursor protein. J Biol Chem 2003;278:34259–67.
[35] Carrotta R, Manno M, Giordano FM, Longo A, Portale G, Martorana V, et al. Protein stability modulated by a conformational effector: effects of trifluoroethanol on bovine serum albumin. Phys Chem Chem Phys 2009;11:4007–18.
[36] Lee YJ, Hirose M. Partially folded state of the disulfide-reduced form of human serum albumin as an intermediate for reversible denaturation. J Biol Chem 1992;267:14753–8.
[37] Sogami M, Ogura S. Structural transitions of bovine plasma albumin. Location of tyrosyl and tryptophyl residues by solvent perturbation difference spectra. J Biochem 1973;73:323–34.
[38] Peters Jr T. All about albumin: biochemistry, genetics and medical applications. CA: Academic Press Inc; 1996. p. 9–54.
[39] Cardamone M, Puri NK. Spectrofluorimetric assessment of the surface hydrophobicity of proteins. J Biochem 1992;282:589–93.
[40] Horowitz PM, Butler M. Interactive intermediates are formed during the urea unfolding of rhodanese. J Biol Chem 1993;268:2500–4.
[41] Deng F, Liu Y. Study of the interaction between tosufloxacin tosylate and bovine serum albumin by multi-spectroscopic methods. J Lumin 2012;132:443–8.
[42] Makhtadze GI, Kim KS, Woodward C. Thermodynamics of BPTI folding. Protein Sci 1993;2:2028–36.
[43] Moriyama Y, Kawasaka Y, Takeda K. Protective effect of small amounts of sodium dodecyl sulfate on the helical structure of bovine serum albumin in thermal denaturation. J Colloid Interface Sci 2003;257:42–6.
[44] Moriyama Y, Watanabe E, Kobayashi K, Harano H, Inui E, Takeda K. Secondary structural change of bovine serum albumin in thermal denaturation up to 130 °C and protective effect of sodium dodecyl sulfate on the protein. J Phys Chem B 2008;112:16585–9.
[45] Timasheff SN, Lee JC, Pittz EP, Tweedy N. The interaction of tubulin and other proteins with structure-stabilizing solvents. J Colloid Interface Sci 1976;55:658–63.
[46] Gekko K, Timasheff SN. Mechanism of protein stabilization by glycerol: preferential hydration in glycerol–water mixtures. Biochemistry 1981;20:4667–76.
[47] Xie G, Timasheff SN. The thermodynamic mechanism of protein stabilization by trehalose. J Biophys Chem 1997;64:25–43.
[48] Timasheff SN. Protein hydration, thermodynamic binding, and preferential hydration. J Biochem 2002;41:13473–82.
[49] Bhat R, Timasheff SN. Steric exclusion is the principal source of the preferential hydration of proteins in the presence of polyethylene glycols. Protein Sci 1992;1:1133–43.
[50] Bolen DW, Baskakov IV. The osmophobic effect: natural selection of a thermodynamic force in protein folding. J Mol Biol 2001;310:955–63.
[51] Qu Y, Bolen CL, Bolen DW. Osmolyte-driven contraction of a random coil protein. Proc Natl Acad Sci USA 1998;95:9268–73.
[52] Back JF, Oakenfull D, Smith MB. Increased thermal stability of proteins in the presence of sugars and polyols. Biochemistry 1979;18:5191–6.
[53] Gerlsma SY. The effects of polyhydric and monohydric alcohols on the heat-induced reversible denaturation of chymotrypsinogen A. Eur J Biochem 1970;14:150–3.
[54] Cottone G, Ciccotti G, Cordone L. Protein–trehalose–water structures in trehalose coated carboxy-myoglobin. J Chem Phys 2002;117:9862–6.
[55] Cottone G. A comparative study of carboxy myoglobin in saccharide-water systems by molecular dynamics simulation. J Phys Chem B 2007;111:3563–9.
[56] Belton PS, Gil AM. IR and Raman spectroscopic studies of the interaction of trehalose with hen egg white lysozyme. Biopolymers 1994;34:957–61.
[57] Schiffer CA, Dotsch V, Wuthrich K, van Gunsteren WF. Exploring the role of the solvent in the denaturation of a protein: a molecular dynamics study of the DNA binding domain of the 434 repressor. Biochemistry 1995;34:15057–67.
[58] Anderson JA. Additive effect of alcohols and polyols on thermostability of pepper leaf extracts. J Am Soc Hort Sci 2007;132:67–72.
[59] Ahmad F, Salahuddin A. Influence of temperature on the intrinsic viscosities of proteins in random coil formation. Biochemistry 1974;13:245–9.
[60] Tamura Y, Gekko K. Compactness on thermally and chemically denatured ribonuclease A as revealed by volume and compressibility. Biochemistry 1995;34:1878–84.
[61] Zoldak G, Zubril A, Musatov A, Stupak M, Sedlak E. Irreversible thermal denaturation of glucose oxidase from *Aspergillus niger* is the thermal transition to the denatured state with residual structure. J Biol Chem 2004;279:47601–9.